Fission Time Scales from Prescisson Charged-Particle Multiplicities

J. P. Lestone, J. R. Leigh, J. O. Newton, D. J. Hinde, J. X. Wei, J. X. Chen,[a] S. Elfstrom, and D. G. Popescu

Department of Nuclear Physics, Research School of Physical Sciences, Australian National University, GPO Box 4, Canberra ACT 2601, Australia

(Received 17 December 1990)

Prescission charged-particle multiplicities, following fusion of ^{164,167,170}Er+^{28}Si, have been measured. The multiplicities at the lowest bombarding energies limit the statistical model level density parameters. More importantly, the α data restrict the time spent near equilibrium and suggest evaporation occurs predominantly from larger deformations.

PACS numbers: 25.70.Jj

The role played by nuclear viscosity or dissipation in the fission process, particularly following heavy-ion fusion, is currently a subject of great interest. The inability of a nucleus to undergo rapidly the large shape changes involved in fission manifests itself in the unexpectedly large number of particles [1–4] and electric-dipole γ rays [5] emitted before scission.

The interpretation of excess particles in terms of the time evolution to scission is an extremely complex problem. However, some insight has been obtained from prescission neutron multiplicities (ν_{pre}) evaluated in terms of a presaddle delay, related to the transient time τ_{tr} required to establish the quasiequilibrium population at the saddle [6], and the time τ_{ssc} to descend from saddle to scission. Particle emission during the presaddle delay is usually assumed to be associated with the equilibrium deformation and affects the fission probability. Within this simple picture a large body of data on ν_{pre} has been used to suggest an overall time scale [2] of order 50×10^{-21} s, although the calculations are insensitive to the individual time regimes. In this Letter we demonstrate that charged-particle multiplicities limit the presaddle delay and offer some hope of better defining the time evolution.

Multiplicities for protons and α particles have been measured for fission of the compound nuclei ^{192}Pb, ^{195}Pb, and ^{198}Pb formed in ^{164,167,170}Er+^{28}Si reactions. The Australian National University 14UD pelletron, operating at voltages up to 15.5 MV, was used to provide 1-ns-wide beam pulses of ^{28}Si ions, every 106 ns, at energies between 140 and 185 MeV. The targets were isotopically enriched, self-supporting foils of $\simeq$700 μg/cm^2 in thickness. Fission fragments were detected in three position-sensitive avalanche detectors, each subdivided into ten regions, and were identified by their energy loss and time of flight relative to the beam pulse. Charged particles were detected in a CsI crystal with a photodiode readout, located at either 90° or 150° to the beam direction, and protons and α's were identified using pulse-shape discrimination. This detector was calibrated using proton and α-particle beams from the 14UD with energies in the range 2–24 and 6–36 MeV, respectively. Thirty particle-fission correlation angles were measured for each particle type and the fission detectors were arranged such that both in- and out-of-plane angles were measured. The geometry is illustrated in Fig. 1.

Multiplicities were extracted from the measured spectra assuming emission from either the compound system prior to fission or from fully accelerated fragments after fission. In the case of α emission it was also necessary to include near-scission emission, a phenomenon well established in low-energy fission [7]. Typical examples of the measured spectra and the fitted components are shown in Fig. 2. The fits to all thirty spectra are good, implying that other sources of emission are not important. The prescission α intensity varies rapidly with spin direction, determined from the fragment direction, and near-scission emission is evident at correlation angles near 90°. The prescission proton and α multiplicities, π_{pre} and α_{pre}, respectively, for ^{192}Pb are shown in Fig. 3 as a function of beam energy. A paper describing details of the experimental methods and analysis is in preparation.

Statistical model calculations were performed using the codes ALERT1 [8], PACE2 [9], and JOANNE [10]. Initially parameters were taken from Ref. [11] where fission cross sections in the $A\sim200$ region were fitted. The level density at equilibrium was taken as $a_\nu=A/10$ MeV^{-1}, that

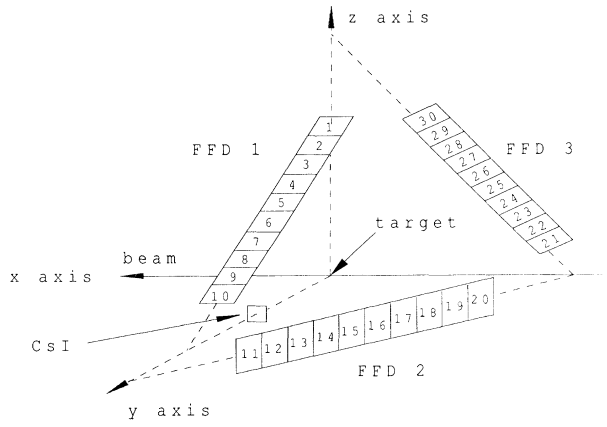

FIG. 1. Schematic arrangement of the fission fragment detectors (FFD) located in three orthogonal planes which intercept at the target.

© 1991 The American Physical Society

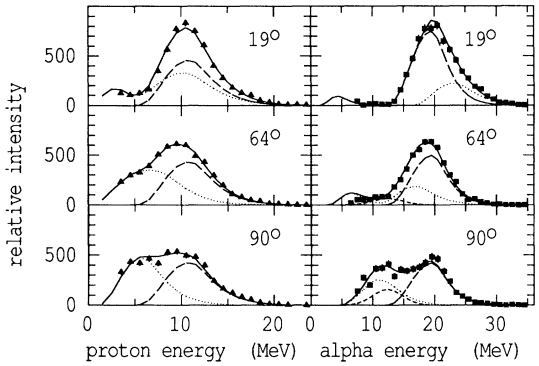

FIG. 2. Representative proton and α-particle spectra, for ^{164}Er+^{28}Si at 177.5 MeV, in coincidence with fission fragments in FFD 1 at the indicated correlation angles. The CsI detector was at 90° to the beam direction. The prescission and postscission components are shown as the dashed and dotted lines, respectively. The short-dashed lines in the α spectra show the near-scission components. The solid lines are the sums of these contributions.

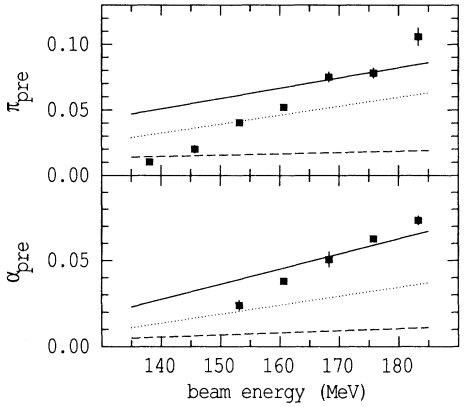

FIG. 3. Statistical model fits to α_{pre} and π_{pre} data for ^{192}Pb, using $a_\nu = A/10$ MeV^{-1}, $a_f/a_\nu = 1.00$ (solid line); $a_\nu = A/7.5$ MeV^{-1}, $a_f/a_\nu = 1.00$ (dotted line); and $a_\nu = A/7.5$ MeV^{-1}, $a_f/a_\nu = 1.05$ (dashed line).

at the saddle point $a_f = a_\nu$, and fission barriers were from the rotating finite range model [12]. The particle transmission coefficients T_l were calculated using "universal" optical model potentials [13,14]. The results of the different codes are consistent with each other. The calculated charged-particle multiplicities overpredict the experimental values at low energies and underestimate them at high energies (see Fig. 3). The discrepancy at low energies cannot be explained in terms of dynamical effects which can only increase the calculated multiplicities. Agreement may be obtained by changing the T_l or the level density parameters. The former are derived from optical model parameters which provide good fits to elastic scattering data from ^{208}Pb at energies near the Coulomb barrier. They are therefore appropriate for spherical nuclei and any changes necessary for hot, rotating nuclei would be expected to *increase* the calculated multiplicities. However, the level density parameters can be used to decrease the multiplicities. Figure 3 illustrates the effect of increasing a_ν to $A/7.5$ MeV^{-1} and then taking $a_f/a_\nu = 1.05$. Hence the low-energy values of π_{pre} are important in limiting the ranges of these parameters.

The values finally used were based on the theoretical values of Ref. [15], where $a_\nu = A/8.6$ MeV^{-1} and a_f/a_ν depends on angular momentum. Values of a_f/a_ν appropriate to the mean fissioning angular momentum were used and varied from 1.08 at 140 MeV to 1.04 at 185 MeV: These values also reproduce the experimental evaporation-residue cross sections [16]. The calculated excitation functions for zero delay times, shown in Fig. 4, are now close to experiment at the lowest energies. However, the data increase with energy considerably more rapidly than the calculations. This behavior is typical of that expected if fission proceeds slowly as a result of dynamical constraints. Contrary to the suggestion of Ref. [17], the α_{pre} data cannot be reproduced without invoking delays to fission.

The Monte Carlo code JOANNE was developed to include, in a simple way, delays to fission in two distinct time regimes: the presaddle region where particle emission competes with fission and the postsaddle region where the nucleus is assumed to be committed to fission and only particle decay is considered.

In the presaddle region statistical decay of the compound nucleus, at its equilibrium deformation and including fission, is calculated using a formalism similar to that

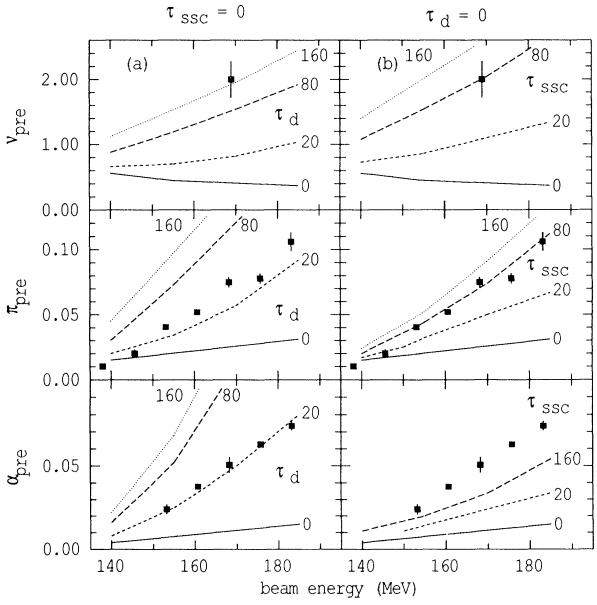

FIG. 4. Comparison of the experimental particle multiplicities for ^{192}Pb with those calculated for (a) various values of τ_d, with $\tau_{ssc} = 0$ and (b) values of τ_{ssc}, with $\tau_d = 0$. The values of τ_d and τ_{ssc} indicated are in units of 10^{-21} s.

of the code PACE2, but each compound-nucleus decay is completed before the next is formed. The fission decay width was taken to be zero up to time τ_d and to have its full statistical model value for longer times, though in reality it would vary more smoothly with time [6] and depend on angular momentum; τ_d would be somewhat shorter than τ_{tr}. The value of α_{pre} increases more rapidly with τ_d than ν_{pre} and π_{pre} because suppression of fission allows emission of particles from states of higher angular momentum, where the yrast line is steeper; α particles can carry more angular momentum than the lighter particles. Typically α_{pre} increases with delay time at about twice the rate of ν_{pre} and π_{pre}, and sets an upper limit to τ_d; an even stricter limit results if T_l's for more deformed systems are used.

In the postsaddle region the nucleus is committed to fission but prescission particles can still be emitted from the composite system during the descent from saddle to scission. The code calculates particle emission, during a time τ_{ssc}, assuming the deformation and rotational energies are equal to the average of those at the saddle point and at scission. A property of the liquid-drop model not generally recognized is that the effective particle binding energies, defined *including* the deformation energy, decrease with increasing deformation for neutrons but increase for charged particles. This is a general result, due mainly to the shape dependence of the Coulomb energy. The tendency is for the binding energies to move towards those of the fragments as scission is approached. For instance, the liquid-drop binding energies for neutrons, protons, and α particles in ^{192}Pb are 8.7, 2.7, and -5.9 MeV, respectively. In the postsaddle region these become 8.4, 4.7, and -2.6 MeV, shifts of -0.3, $+2.0$, and $+3.3$ MeV. A change in binding energy of 1 MeV typically changes the particle decay width by a factor of 2. Thus the increase in deformation results in the suppression of α's, relative to neutron emission, by more than an order of magnitude. Now, in contrast to the presaddle region, the maximum delay time τ_{ssc} is limited by ν_{pre}.

The fission delay times required to reproduce the observed multiplicities have been calculated with JOANNE and are illustrated in Fig. 4 for the reaction ^{164}Er+^{28}Si. For $\tau_{ssc}=0$, the α_{pre} and π_{pre} excitation functions are well reproduced with $\tau_d=20\times10^{-21}$ s whereas ν_{pre} requires delays almost an order of magnitude larger. It is not possible to obtain a consistent description of the data if particle emission occurs only from the nucleus at or near its equilibrium deformation, as assumed in the calculation. For $\tau_d=0$ the ν_{pre} and π_{pre} are consistent with $\tau_{ssc}\simeq80\times10^{-21}$ s whereas α_{pre} requires values in excess of 200×10^{-21} s. The allowed values of τ_{ssc} could be made more compatible by the use of deformed T_l values.

The combinations of τ_d and τ_{ssc} giving acceptable fits to each of the observed multiplicities are shown in Fig. 5. All multiplicities can be reproduced with values of τ_d and τ_{ssc} of $\sim10\times10^{-21}$ and $\sim50\times10^{-21}$ s, respectively. Figure 6 shows the comparison between experiment and calculation for ^{192}Pb and ^{198}Pb using this combination of delays. The variation of all multiplicities with bombarding energy and target mass is well reproduced; the overall agreement is excellent. Thus our analysis suggests that the overall fission time scale is $\sim60\times10^{-21}$ s and τ_d is limited to $\sim10\times10^{-21}$ s.

The value of τ_{scc} is almost an order of magnitude longer than theoretical estimates [18]. However, it is unwise to interpret our times, derived from a very simple model, in terms of the transient delay and saddle-to-scission time. Nevertheless they each suggest that parti-

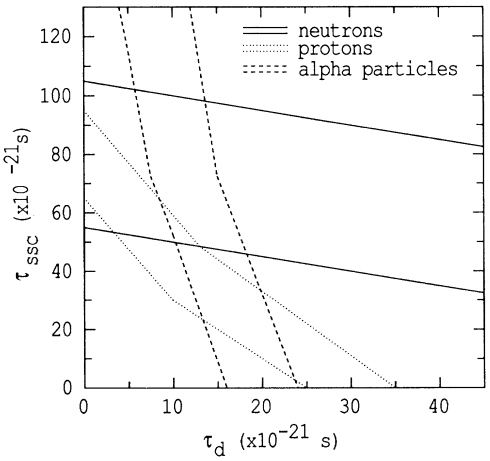

FIG. 5. Combinations of τ_d and τ_{ssc} required to provide acceptable fits to the measured particle multiplicities for ^{192}Pb. The separations of similar lines relate to the experimental errors.

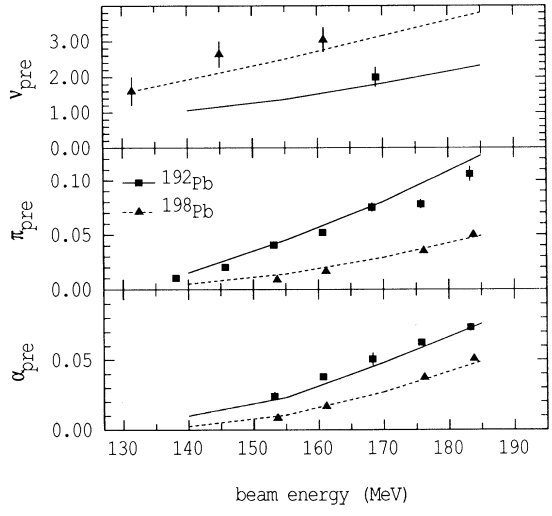

FIG. 6. Measured multiplicities for ^{192}Pb (squares) and ^{198}Pb (triangles). The calculated curves for ^{192}Pb (solid line) and ^{198}Pb (dashed line) use $\tau_d=10\times10^{-21}$ s and $\tau_{ssc}=50\times10^{-21}$ s.

cle emission originates predominantly from nuclei with deformations significantly larger than the equilibrium value. This conclusion would not be affected if values of T_l appropriate to deformed nuclei were used.

A detailed interpretation of the data must await the development of sophisticated models which combine evaporation with dynamics. The apparent sensitivity to deformation of the different evaporated particles will be a useful test of any such development.

---

[a]Present address: Institute of Heavy Ion Physics, Peking University, Beijing, People's Republic of China.

[1] A. Gavron *et al.*, Phys. Rev. C **35**, 579 (1987).
[2] D. J. Hinde *et al.*, Nucl. Phys. **A502**, 497c (1989), and references therein.
[3] B. Lindl *et al.*, Z. Phys. A **328**, 85 (1987).
[4] G. F. Peaslee *et al.*, Phys. Rev. C **38**, 1730 (1988).
[5] M. Thoennessen *et al.*, Phys. Rev. Lett. **59**, 2860 (1987).
[6] P. Grangé *et al.*, Phys. Rev. C **27**, 2063 (1983).
[7] J. P. Theobald *et al.*, Nucl. Phys. **A502**, 343c (1989); A. K. Sinha *et al.*, Pramana **33**, 85 (1989).
[8] M. Blann and T. T. Komoto, Phys. Rev. C **26**, 472 (1982).
[9] A. Gavron, Phys. Rev. C **21**, 230 (1980).
[10] J. P. Lestone, Ph.D. thesis, Australian National University, 1990, and Internal Report No. ANU/P1084 (unpublished).
[11] R. J. Charity *et al.*, Nucl. Phys. **A457**, 441 (1986); J. O. Newton *et al.*, Nucl. Phys. **A483**, 126 (1988).
[12] A. J. Sierk, Phys. Rev. C **33**, 2039 (1986).
[13] C. M. Perey and F. G. Perey, At. Data Nucl. Data Tables **17**, 1 (1976).
[14] J. R. Huizenga and G. Igo, Nucl. Phys. **29**, 462 (1962).
[15] J. Töke and W. J. Swiatecki, Nucl. Phys. **A372**, 141 (1981).
[16] D. J. Hinde *et al.*, Nucl. Phys. **A398**, 308 (1983).
[17] H. Ikeoze *et al.*, Phys. Rev. C **42**, 342 (1990).
[18] J. R. Nix, Nucl. Phys. **A502**, 609c (1989), and references therein.